Neoplasma 2022; 69(5): 1079–1091

doi:10.4149/neo_2022_220225N209

hsa_circ_0067514 suppresses gastric cancer progression and glycolysis via miR-654-3p/LATS2 axis

Shao-Feng JIANG, Rong-Rong LI*

Department of Medical Oncology-Gastroenterology and Urology, Hunan Cancer Hospital, The Affiliated Cancer Hospital of Xiangya School of Medicine, Central South University, Changsha, Hunan, China

**Correspondence: lirongrongxiangya@126.com*

Received February 25, 2022 / Accepted June 23, 2022

Gastric cancer is the third most frequent cancer with high prevalence and mortality globally. Circular RNAs (circRNAs) play a key role in cancer regulation, including gastric cancer. Nevertheless, only a few circRNAs have been well elucidated in gastric cancer. Hence, we investigated the action of circ_0067514 on gastric cancer and clarified the underlying mechanism. Here, we found that circ_0067514 was decreased in gastric cancer patients and cancer cells. The circ_0067514 expression was correlated with gastric cancer overall survival, lymph node metastasis, tumor, node, metastasis (TNM) stage, and histological differentiation. Overexpression of circ_0067514 blocked proliferation, invasion, and glycolysis of gastric cancer cells. Besides, circ_0067514 regulated large tumor suppressor kinase 2 (LATS2) expression by absorbing microRNA (miR)-654-3p. Furthermore, circ_0067514 modulated gastric cancer aggressive behaviors and glycolysis via miR-654-3p/LATS2 axis. Moreover, circ_0067514 constrained tumor growth in vivo. Together, this study showed that circ_0067514 suppressed gastric cancer aggressive development and glycolysis via miR-654-3p/LATS2 axis, making circ_0067514 a valuable target for preventing gastric cancer progression.

Key words: circ_0067514, miR-654-3p, LATS2, gastric cancer, invasion, glycolysis

Gastric cancer is the third most frequent cancer with high prevalence and mortality globally [1, 2]. Over a million cases are diagnosed each year worldwide [3, 4]. In 2018, more than 782,000 cases died of gastric cancer [4, 5]. Due to the lack of associated symptoms and screening methods, gastric cancer cases are always diagnosed at the last stage [1, 5, 6]. Unfortunately, the conventional treatment is not curative for advanced gastric cancer. Despite tremendous efforts, no significant improvement has been achieved in terms of curative treatment [1, 7]. The median survival of advanced gastric cancer patients is 8–11 months [8, 9]. Therefore, further identifying the development mechanism in gastric cancer is of great importance for therapy.

Circular RNAs (circRNAs) play key roles in various biological functions, including RNA-binding protein (RBP) sponges, gene transcription, RNA splicing regulators, especially as microRNA (miRNA) sponges [10]. circRNAs contain multiple miRNA response elements (MERs), which allow circRNAs to act as competitive endogenous RNAs (ceRNAs) to target miRNAs and thereby modify downstream gene expression [11]. Recently, circRNAs are known to exert a regulatory effect in cancers [12]. For example, circMET fuels anti-programmed cell death protein 1 (PD1) treatment resistance in hepatocellular carcinoma through the miR-30-5p/snail/dipeptidyl peptidase 4 (DPP4) axis [13]. hsa_circRNA_100146 drives prostate cancer progression by serving as the miR-615-5p sponge and thereby elevates thyroid hormone receptor interactor 13 (TRIP13) expression [14]. Similarly, increasing evidence suggests the modulation role of circRNAs in gastric cancer [15, 16]. For instance, circNRIP1 serves as a miR-149-5p sponge to potentiate gastric cancer aggressive phenotype through modulating the AKT serine/threonine kinase 1 (AKT1)/mammalian target of rapamycin (mTOR) pathway [15]. circCUL2 regulates gastric cancer malignant development and cisplatin sensibility via miR-142-3p/Rho-associated coiled-coil containing kinase isoform 2 (ROCK2) axis [16]. As a member of circRNAs, hsa_circ_0067514, forms from host gene centrosomal protein 70 (CEP70) and locates on chromosome 13, is downregulated in gastric cancer based on the analytical results of the Gene Expression Omnibus (GEO) database. However, its role in gastric cancer remains elusive.

Emerging studies show that miRNAs modulate the target gene expression, thereby regulating gastric cancer progression [17, 18]. For example, miR-877-5p suppresses gastric cancer cell proliferation by targeting Forkhead Box M1 (FOXM1) [17]. miR-452 promotes the development of gastric cancer via binding Erythrocyte Band 4.1-like protein 3 (EPB41L3) [18]. It is accepted that circRNAs are the upstream regulators of miRNAs via acting as ceRNAs [19]. The member of miRNAs, miR-654-3p, is located on chromosome 14 and participates in gastric cancer malignant behaviors [20]. Furthermore, miR-654-3p is a potential target of hsa_circ_0067514. Therefore, hsa_circ_0067514 may be involved in gastric cancer progression via the ceRNA mechanism to absorb miR-654-3p.

Thus, this research systematically investigated the action of hsa_circ_0067514 on gastric cancer and clarified the precise mechanism.

Patients and methods

Patient tissue samples. Resected tumor tissues and paired adjacent normal tissues were harvested from 80 gastric patients in Hunan Cancer Hospital. No patients had undergone preoperative chemotherapy or radiotherapy. All patients signed informed consent. The Ethics Committee of Hunan Cancer Hospital authorized this research.

Cell culture. Human gastric epithelial cell line (GES-1), and gastric cancer cell lines AGS and HGC-27, were obtained from BeNa Culture Collection (BeNa, Beijing, China). All cells were grown in DMEM supplemented with 10% fetal bovine serum (FBS) and 1% streptomycin/penicillin (Thermo Fisher Scientific, MA, USA) at 37°C with 5% CO_2.

Quantitative real-time polymerase chain reaction (qRT-PCR). RNA samples were isolated using the TRIzol reagent (TIANGEN, Beijing, China). Cytoplasmic and nuclear RNA were separated using the PARIS Kit (Thermo Fisher Scientific, MA, USA). These RNAs were transcribed into complementary DNA (cDNA) using the cDNA Synthesis Kit and TaqMan MicroRNA Reverse Transcription Kit (Thermo Fisher Scientific, MA, USA). qPCR assay was conducted using SYBR Green Master Mix (Thermo Fisher Scientific, MA, USA) following the supplier's protocol. The primer sequences were: hsa_circ_0067514, F: 5'-CAGGCCTACGCAGCATGAAT-3', R: 5'-CCAGGTTAGGCTGGGATCAG-3'; miR-654-3p, F: 5'-TCGGCAGGTGGTGGGCCGCAG-3', R: 5'-CACTCAACTGGTGTCGTGGA-3' [21]; large tumor suppressor kinase 2 (LATS2), F: 5'-AGCTGGACTCTGTGAAGCTG-3', R: 5'-TGTCCACCTTACAAGCAAGG-3' [22]. *GAPDH* and *U6* were used as control genes. Relative expression was quantified using the $2^{-\Delta\Delta Ct}$ method. The experiment was repeated three times.

Cell transfection. The miR-654-3p mimic (Cat. # miR10004814-1-5), siRNA target LATS2 (si-LATS2) (si-LATS2#1: 5'-CAGAAAGCCTTGAGGGAAATCAGAT-3'; si-LATS2#2: 5'-GCCTCAACGTGGACCTGTATGAATT-3'), and negative controls were synthesized by RiboBio (RiboBio, Guangzhou, China). The empty vector of pLCDH-circRNA was purchased from Geneseed (Cat. No. GS0104, Geneseed, Guangzhou, China). The sequence of circ_0067514 was amplified and pLCDH-circ_0067514 was constructed by RiboBio (RiboBio, Guangzhou, China). Transfections of these vectors were conducted using Lipofectamine 3000 (Thermo Scientific, MA, USA) following the supplier's protocol. The experiment was repeated three times.

Cell counting kit 8 (CCK-8) assays. AGS and HGC-27 cells were grown in 96-well plates (10^4 cells/well) for 24 h, 48 h, and 72 h, respectively. CCK-8 reagent (10 μl, Sigma, MO, USA) was added to cells for 4 h. The optical density at 450 nm was observed utilizing the microplate reader (Bio-Tek EPOCH2, VT, USA). The assay was repeated three times.

EdU staining. BeyoClick EdU Cell Proliferation Kit with Alexa Fluor 594 (Beyotime Biotechnology, Shanghai, China) was employed to assess proliferation according to the supplier's protocols. AGS and HGC-27 cells were stained with 10 μM of EdU for 3 h. Cells were immobilized by fixative reagent and treated by permeate reagent for 15 min respectively, followed by incubating with Click Additive Solution for 30 min without light. Cells nuclei were dyed with 4',6-diamidino-2-phenylindole (DAPI). The staining images were acquired using the fluorescent microscope, and the proportion of EdU-positive cells was analyzed. The experiment was repeated three times.

Transwell invasion assay. Invasion assay was performed using Transwell chambers (BD Biosciences, NJ, USA) overlaid with Matrigel. The cell suspension was prepared and inoculated into the top chamber with the medium without serum. The bottom chamber was filled with a complete medium. After 24 h of cultivation, the invaded cells were immobilized and dyed with crystal violet for 15 min. The images were obtained using the microscope. The assay was repeated three times.

Western blot. Protein samples were harvested from cells using RIPA reagent (TIANGEN, Beijing, China), and concentration determination was performed by the BCA method. Protein lysates were size-fractionated on SDS-PAGE and transferred onto the PVDF membranes. After blocking non-specific interactions, western blot analyses were conducted using primary antibodies including ant-Ki-67 (1:1000, ab231172, Abcam), anti-E-cadherin (1:1000, ab40772, Abcam), anti-N-cadherin (1:2000, ab76011, Abcam), anti-hexokinase-2 (HK-2, 1:2000, ab209847, Abcam), anti-lactate dehydrogenase A (LDHA, 1:1000, ab52488, Abcam), anti-LATS2 (1:1000, ab243657, Abcam) and anti-β-actin (1:5000, ab6276, Abcam) antibodies. After the washing step, the membranes were treated with IgG H&L (HRP, 1:3000, ab6721, Abcam). The blots were measured by the ECL chemiluminescence system and quantified using ImageJ. The experiment was repeated three times.

Determination of glucose uptake, lactate production, and adenosine triphosphate (ATP) level. Determination

of glucose absorption, lactate formation, and ATP level was carried out using Glucose Uptake Assay Kit, Lactate ELISA Kit (Abcam), and Enhanced ATP assay kit (Beyotime, Shanghai, China) according to the supplier's protocols. The experiment was repeated three times.

Luciferase assay. The wild and mutant sequences of hsa_circ_0067514 binding to miR-654-3p and 3' untranslated regions (3'-UTR) of LATS2 were cloned into the pGL3 luciferase vector (Promega, WI, USA), respectively. The cloned pGL3 plasmids and miR-654-3p mimics were co-transfected into AGS and HGC-27 cells. Luciferase activity was recorded using the Dual-luciferase reporter assay system (Promega). The assay was repeated three times.

RNA pull-down. Biotinylated negative control (Bio-NC) and miR-654-3p (Bio-miR-654-3p) were generated in RiboBio (Ribobio, Guangzhou, China). The Bio-NC and Bio-miR-654-3p were transfected into cells, respectively. Cells were lysed after 48 h and lysates were probed with magnetic beads. After the washing step, the absorbed RNAs were obtained and measured using qRT-PCR. The experiment was repeated three times.

RNA immunoprecipitation (RIP). RIP assay was conducted using the RNA-Binding Protein Immunoprecipitation Kit (Millipore, MA, USA) in line with the supplier's protocols. The cell lysates were immunoprecipitated using the Ago2 antibody (ab186733, Abcam). The abundances of hsa_circ_0067514 and miR-654-3p were determined using qRT-PCR. The assay was repeated three times.

Establishment of xenograft tumor. To establish xenograft tumor, 10 BALB/c nude mice aged 6 weeks were acquired from Beijing Laboratory Animal Research Center (Beijing, China) and allocated into the pLCDH-cir group and the pLCDH-circ_0067514 group. AGS cells were transfected into pLCDH-cir or pLCDH-circ_0067514. All mice received 5×10^6 AGS cells via subcutaneous injection. Five days later, tumor volumes were monitored every 5 days. Thirty days later, all mice were euthanized with CO_2 inhalation, and tumors were dissected to perform qRT-PCR and immunohistochemistry. The experiments complied with the national and international regulations and policies, and the Ethics Committee of Hunan Cancer Hospital authorized the study.

Immunohistochemistry. After mice were euthanized, the tumors were dissected, fixed, embedded, and prepared into 5 μm section samples. The sections were deparaffinized, rehydrated, blocked endogenous peroxidase activity and non-specific binding, followed by probing with the primary antibodies including Ki-67 (1:200, ab231172, Abcam), LATS2 (1:200, PA5-120433, Thermo Scientific, MA, USA), E-cadherin (1:200, PA5-85088, Thermo Scientific), N-cadherin (1:200, ab76011, Abcam), HK2 (1:200, ab209847, Abcam), LDHA (1:200, ab52488, Abcam) at 4°C overnight. After that, the slices were incubated with IgG H&L (HRP) (1:1000, ab6721, Abcam) and dyed with the DAB (R&D Systems, MN, USA). The images were obtained using the microscope. The experiment was repeated three times.

Statistical analysis. Data were represented by mean ± standard deviation (SD), and statistical significance was conducted using SPSS Statistics 22.0 (SPSS, Chicago, IL, USA). The difference between tumor tissues and paired normal tissues was evaluated by the paired t-test. Student's t-test was used for analyzing the significance between the two groups. One-way ANOVA was applied to determine the significance between multiple groups. Kaplan-Meier analysis with the log-rank test analyzed the survival of patients. A p-value <0.05 was considered as statistically significant.

Results

circ_0067514 is low expressed in gastric cancer. To elucidate the role of circ_0067514 in gastric cancer, the circ_0067514 expression was initially determined. According to the analytical results of GSE184882, circ_0067514 was lowly expressed in gastric cancer ($p<0.001$, Figure 1A). Afterward, we detected the circ_0067514 expression in cancer tissues of 80 gastric cancer patients using qRT-PCR. It was observed that circ_0067514 was declined in cancer tissues ($p<0.001$, Figure 1B). Interestingly, the overall survival of patients with low expression of circ_0067514 was poor ($p<0.05$, Figure 1C). The circ_0067514 expression was correlated with lymph node metastasis, TNM stage, and histological differentiation in gastric cancer ($p<0.05$, Table 1). Furthermore, circ_0067514 was declined in gastric cancer cells ($p<0.01$, Figure 1D). The structure and junction sites of circ_0067514 are listed in Figure 1E. Next, the stability

Table 1. Correlation between circ_0067514 expression and the clinical pathological features of 80 gastric cancer patients.

Characteristic	All cases	circ_0067514 expression		p-value
		High (n=40)	Low (n=40)	
Age (years)				0.502
<60	39	18	21	
≥60	41	22	19	
Gender				0.818
Female	31	16	15	
Male	49	24	25	
Tumor size (cm)				0.366
<3	34	15	19	
≥3	46	25	21	
Lymph node metastasis				0.015*
Yes	44	30	14	
No	36	10	26	
TNM				0.007*
I+II	36	24	12	
III+IV	44	16	28	
Differentiation				0.014*
Well and Moderate	37	24	13	
Poor	43	16	27	

*p<0.05

of circ_0067514 was verified using RNase R. RNase R treatment inhibited the level of linear CEP70 mRNA but had no effect on circ_0067514 level ($p<0.01$, Figure 1F). Moreover, circ_0067514 was mainly localized in the cytoplasm ($p<0.01$, Figure 1G). Therefore, circ_0067514 was lowly expressed in gastric cancer.

Enforced circ_0067514 constrains the proliferation, invasion, and epithelial-mesenchymal transition (EMT) of gastric cancer cells. To study the action of circ_0067514 on gastric cancer, pLCDH-circ_0067514 was transfected into AGS and HGC-27 cells. pLCDH-circ_0067514 significantly enhanced the expression of circ_0067514 ($p<0.001$, Figure 2A). Next, the influence of elevated circ_0067514 on gastric cancer progression was detected. We found that circ_0067514 overexpression blocked gastric cancer cell viability, proliferation, and invasion ability ($p<0.01$, Figures 2B-2D). Overexpression of circ_0067514 also inhibited the levels of Ki-67 and N-cadherin and enhanced the E-cadherin level ($p<0.01$, Figure 2E). Thus, overexpression of circ_0067514 constrained gastric cancer proliferation, invasion, and EMT.

Overexpression of circ_0067514 suppresses glycolysis in gastric cancer. Additionally, the action of circ_0067514 on glycolysis was detected. We found that circ_0067514 overexpression significantly suppressed the glucose absorption, lactate formation, and ATP level of gastric cancer cells

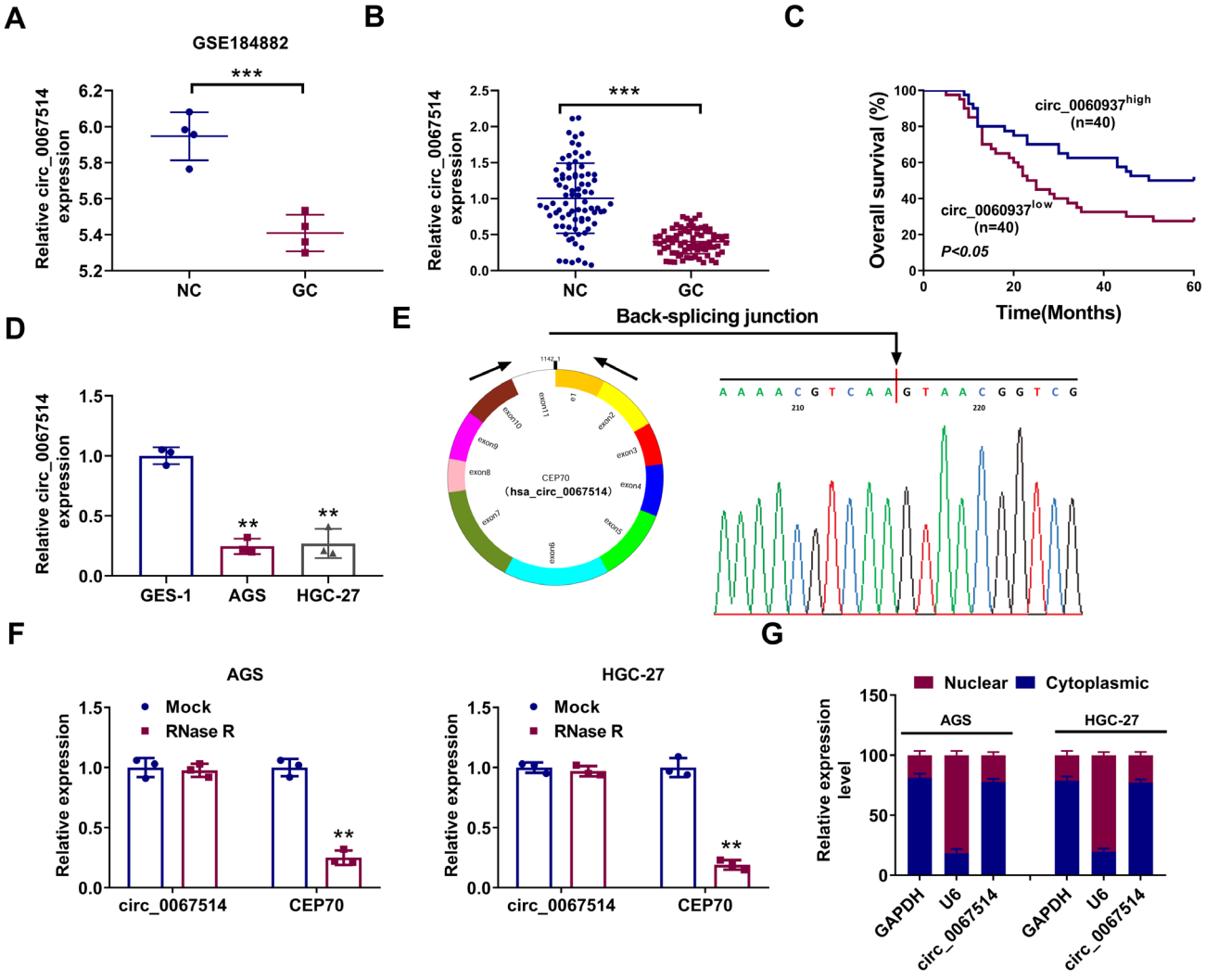

Figure 1. circ_0067514 is downregulated in gastric cancer. A) The expression of circ_0067514 was analyzed using the data of GSE184882. ***p<0.001 versus the NC group. B) circ_0067514 expression in 80 gastric cancer patients was determined using qRT-PCR. ***p<0.001 versus the NC group. C) The association between circ_0067514 expression and overall survival of gastric cancer patients was analyzed by Kaplan-Meier analysis. D) circ_0067514 expression in gastric epithelial cell line GES-1 and gastric cancer cell lines AGS and HGC-27 were determined using qRT-PCR. **p<0.01 versus the GES-1 group. E) The structure and junction sites of circ_0067514 were presented. F) The stability of circ_0067514 after treatment with RNase R was determined using qRT-PCR. **p<0.01 versus the Mock group. G) The distribution of circ_0067514 in the cytoplasm and nucleus was evaluated by qRT-PCR.

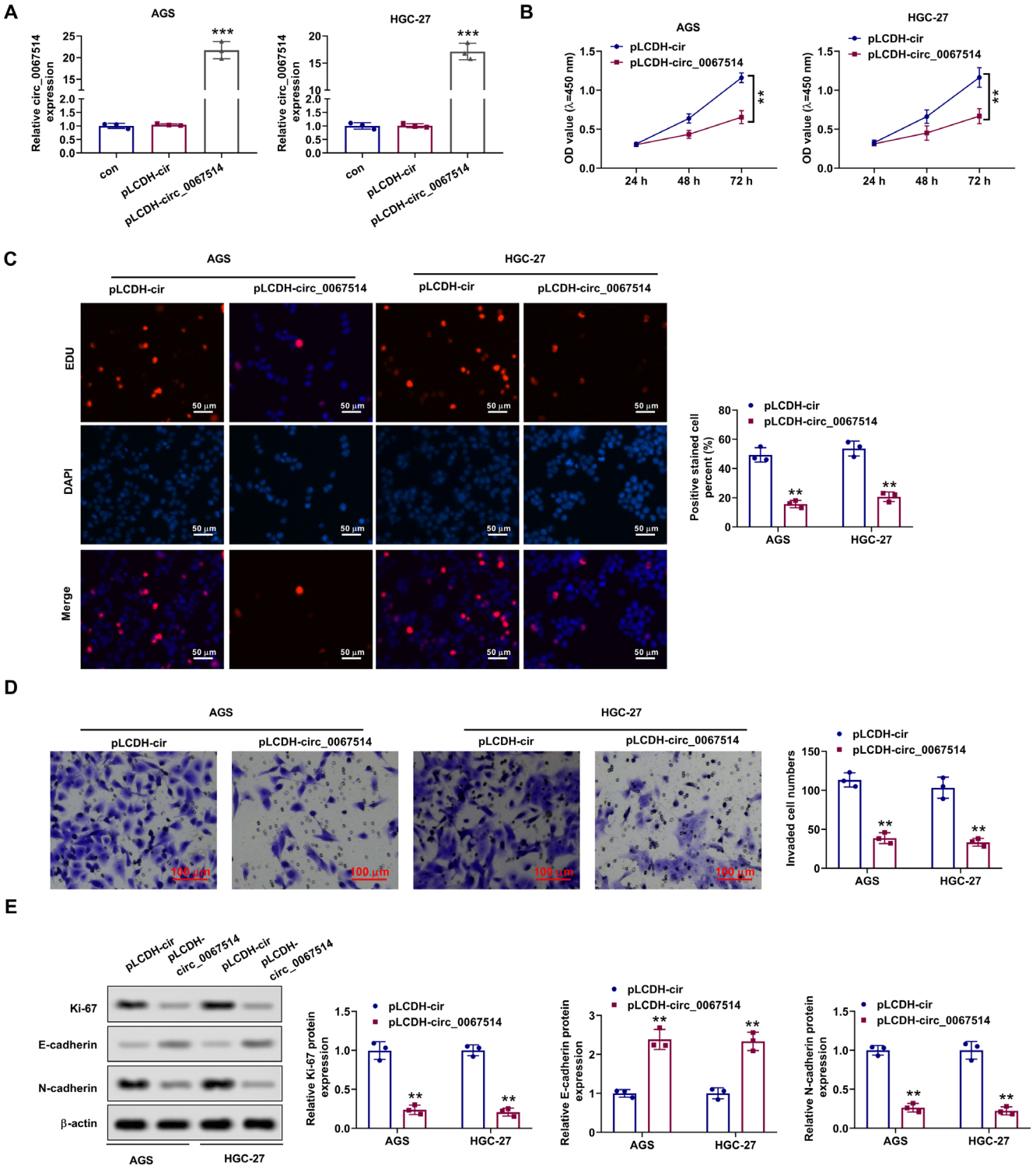

Figure 2. Overexpression of circ_0067514 suppresses the proliferation, migration, and invasion of gastric cancer cells. A) The expression of circ_0067514 was measured using qRT-PCR in AGS and HGC-27 cells after transfection with pLCDH-circ_0067514. B) CCK-8 assay assessed the cell viability of AGS and HGC-27 cells after transfection with pLCDH-circ_0067514. C) EdU staining determined the proliferation ability of AGS and HGC-27 cells after transfection with pLCDH-circ_0067514. D) Transwell invasion assay detected the invasion ability of AGS and HGC-27 cells after transfection with pLCDH-circ_0067514. E) The protein levels of Ki-67, E-cadherin, and N-cadherin in AGS and HGC-27 cells after transfection with pLCDH-circ_0067514 were detected by western blot. **p<0.01; ***p<0.001 versus the pLCDH-cir group.

(p<0.01, Figures 3A–3C). The levels of HK2 and LDHA were also inhibited by elevated circ_0067514 (p<0.01, Figure 3D). Hence, overexpression of circ_0067514 suppressed glycolysis of gastric cancer cells.

circ_0067514 acts as a miR-654-3p sponge. To clarify the downstream mechanism of circ_0067514 on gastric cancer, the potential target miRNA of circ_0067514 was browsed in CircInteractome and found that circ_0067514 may target miR-654-3p. The speculative targeting sites between circ_0067514 and miR-654-3p are presented in Figure 4A. To validate the relationship between circ_0067514 and miR-654-3p, miR-654-3p mimic was transfected into gastric cancer cells to elevate the miR-654-3p expression (p<0.01, Figure 4B). In addition, the luciferase assay proved that miR-654-3p mimic decreased the reporter activity of wild circ_0067514 but had no influence on the reporter activity of mutant circ_0067514 (p<0.01, Figure 4C). As expected, RNA pull-down and RIP assay also confirmed the targeting relationship between circ_0067514 and miR-654-3p (p<0.01, Figures 4D, 4E). Notably, miR-654-3p exhibited overt elevation in gastric cancer tissues (p<0.001, Figure 4F). The miR-654-3p expression was negatively related to the expression of circ_0067514 (p<0.001, Figure 4G). Furthermore, miR-654-3p also was elevated in gastric cancer cells (p<0.01, Figure 4H). Moreover, overexpression of circ_0067514 suppressed the miR-654-3p expression (p<0.01, Figure 4I). These findings verified that circ_0067514 served as a miR-654-3p sponge.

miR-654-3p targets LATS2. miRNAs usually exert functions by targeting mRNAs. We, therefore, screened the target mRNA of miR-654-3p in Target Scan and found that LATS2 was a potential target of miR-654-3p. The predictive targeting sequences between miR-654-3p and LATS2 are presented in Figure 5A. To validate the relationship between miR-654-3p and LATS2, the luciferase assay was conducted and demonstrated that miR-654-3p mimic decreased the reporter activity of wild LATS2 3'-UTR but had no effect on the reporter activity of mutant LATS2 3'-UTR (p<0.01, Figure 5A). Additionally, miR-654-3p mimic inhibited the LATS2 expression (p<0.01, Figure 5B). LATS2 was decreased in gastric cancer tissues (p<0.001, Figure 5C). The LATS2 expression was inversely related to miR-654-3p and positively related to circ_0067514 (p<0.001, Figure 5D, 5E). Furthermore, the LATS2 also was downregulated in gastric cancer cells (p<0.01, Figure 5F). Collectively, miR-654-3p targeted LATS2.

circ_0067514 regulates gastric cancer malignant development via miR-654-3p/LATS2 axis. Given the relationship among circ_0067514, miR-654-3p, and LATS2, we reasoned that circ_0067514 might regulate gastric cancer progression via the miR-654-3p/LATS2 axis. To this end, si-LATS2 was initially transfected into AGS and HGC-27 cells, and knockdown efficiency was confirmed using western blot (p<0.05, Figure 6A). Next, the LATS2 levels in cells after co-transfected with pLCDH-circ_0067514 and miR-654-3p mimic or si-LATS2 were determined by western blot. Results revealed

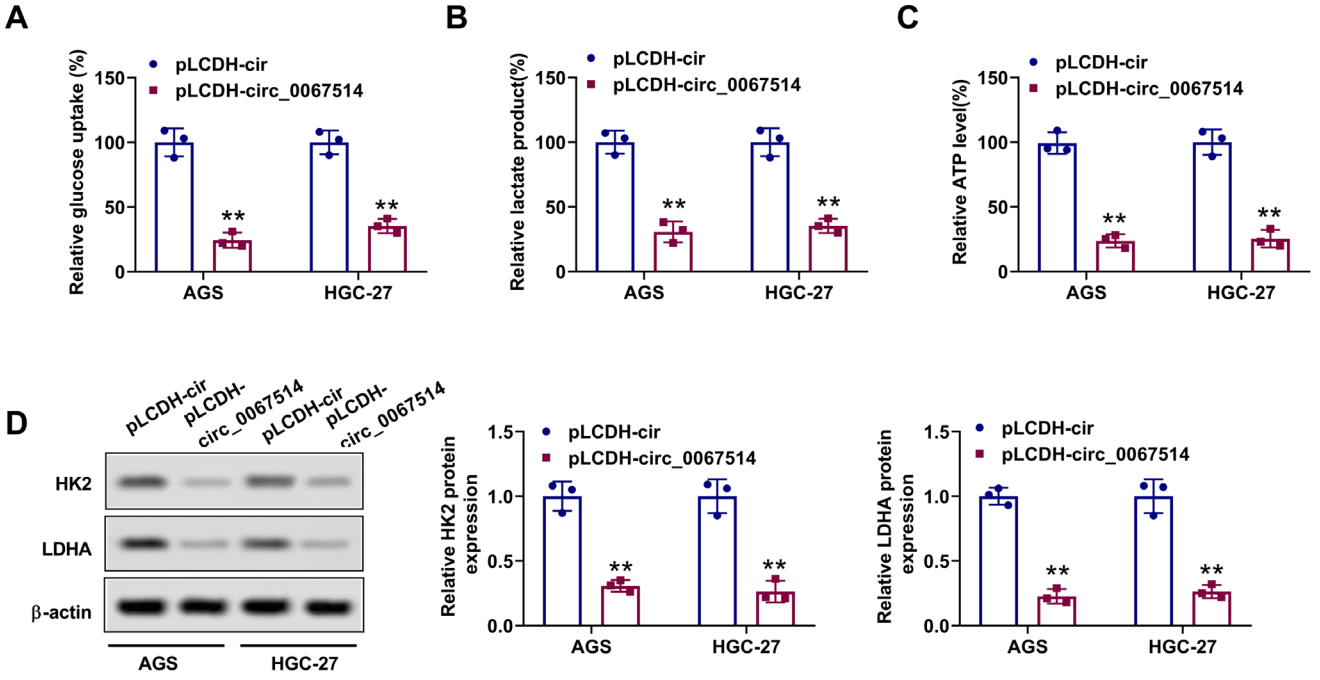

Figure 3. Overexpression of circ_0067514 suppresses glycolysis of gastric cancer cells. A) The glucose uptake of AGS and HGC-27 cells transfected with pLCDH-circ_0067514 was measured. B) The lactate production of AGS and HGC-27 cells after transfection with pLCDH-circ_0067514 was assessed. C) The ATP level of AGS and HGC-27 cells after transfection with pLCDH-circ_0067514 was evaluated. D) The protein levels of HK2 and LDHA in AGS and HGC-27 cells after transfection with pLCDH-circ_0067514 were measured by western blot. **p<0.01 versus the pLCDH-cir group.

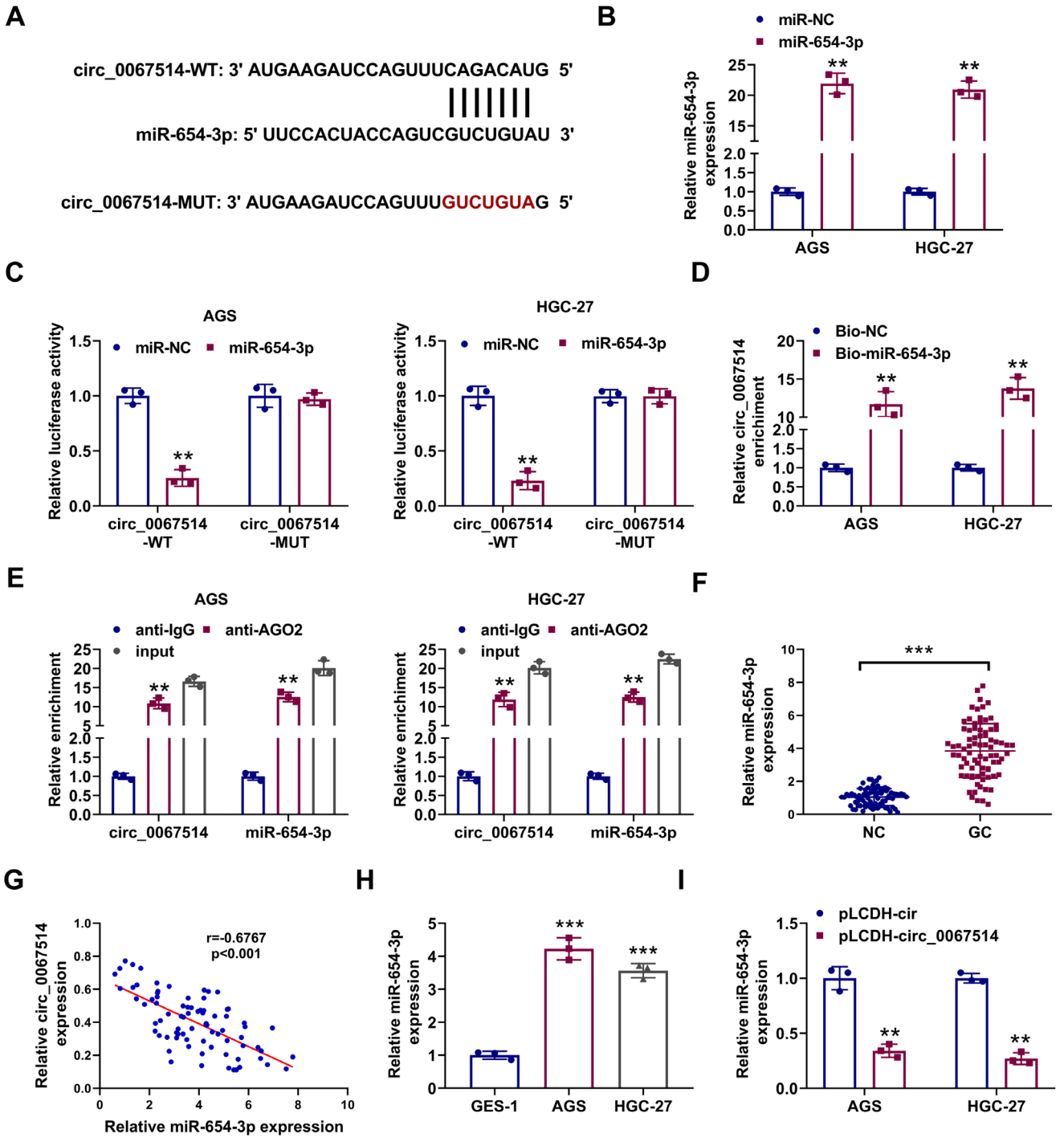

Figure 4. circ_0067514 acts as a miR-654-3p sponge. A) The putative targeting sites between circ_0067514 and miR-654-3p were presented. B) The expression of miR-654-3p was determined by qRT-PCR in AGS and HGC-27 cells after transfection with miR-654-3p mimic. **p<0.01 versus the miR-NC group. C) The relationship between circ_0067514 and miR-654-3p was determined by the luciferase assay. **p<0.01 versus the miR-NC group. D) The relationship of circ_0067514 and miR-654-3p was determined by RNA pull-down. **p<0.01 versus the Bio-NC group. E) The relationship between circ_0067514 and miR-654-3p was determined by the RIP assay. **p<0.01 versus the anti-IgG group. F) The expression of miR-654-3p in 80 gastric cancer patients was determined by qRT-PCR. ***p<0.001 versus the NC group. G) The association between the expression of circ_0067514 and miR-654-3p was analyzed by Pearson's correlation coefficient. H) The expression of miR-654-3p in GES-1, AGS, and HGC-27 cells was determined using qRT-PCR. ***p<0.001 versus the GES-1 group. I) The expression of miR-654-3p in AGS and HGC-27 cells after transfection with pLCDH-circ_0067514 was detected by qRT-PCR. **p<0.01 versus the pLCDH-cir group.

that circ_0067514 overexpression elevated the expression of LATS2 but was reversed by miR-654-3p mimic and si-LATS2 ($p<0.05$, Figures 6B, 6C). Further functional experimental findings revealed that the inhibitory effects of overexpressed circ_0067514 on gastric cancer viability, proliferation, and invasion ability were restored by miR-654-3p mimic and si-LATS2 ($p<0.05$, Figures 6D–6G). Furthermore, overexpressed circ_0067514 inhibited the levels of Ki-67 and N-cadherin and increased the E-cadherin level, which was abrogated by miR-654-3p mimic and si-LATS2 ($p<0.05$, Figure 6H). In general, circ_0067514 regulated gastric cancer malignant behaviors via miR-654-3p/LATS2 axis.

circ_0067514 blocks tumor growth of gastric cancer *in vivo*. To investigate the role of circ_0067514 in gastric cancer progression *in vivo*, a xenograft tumor was established using AGS cells transfected with pLCDH-circ_0067514.

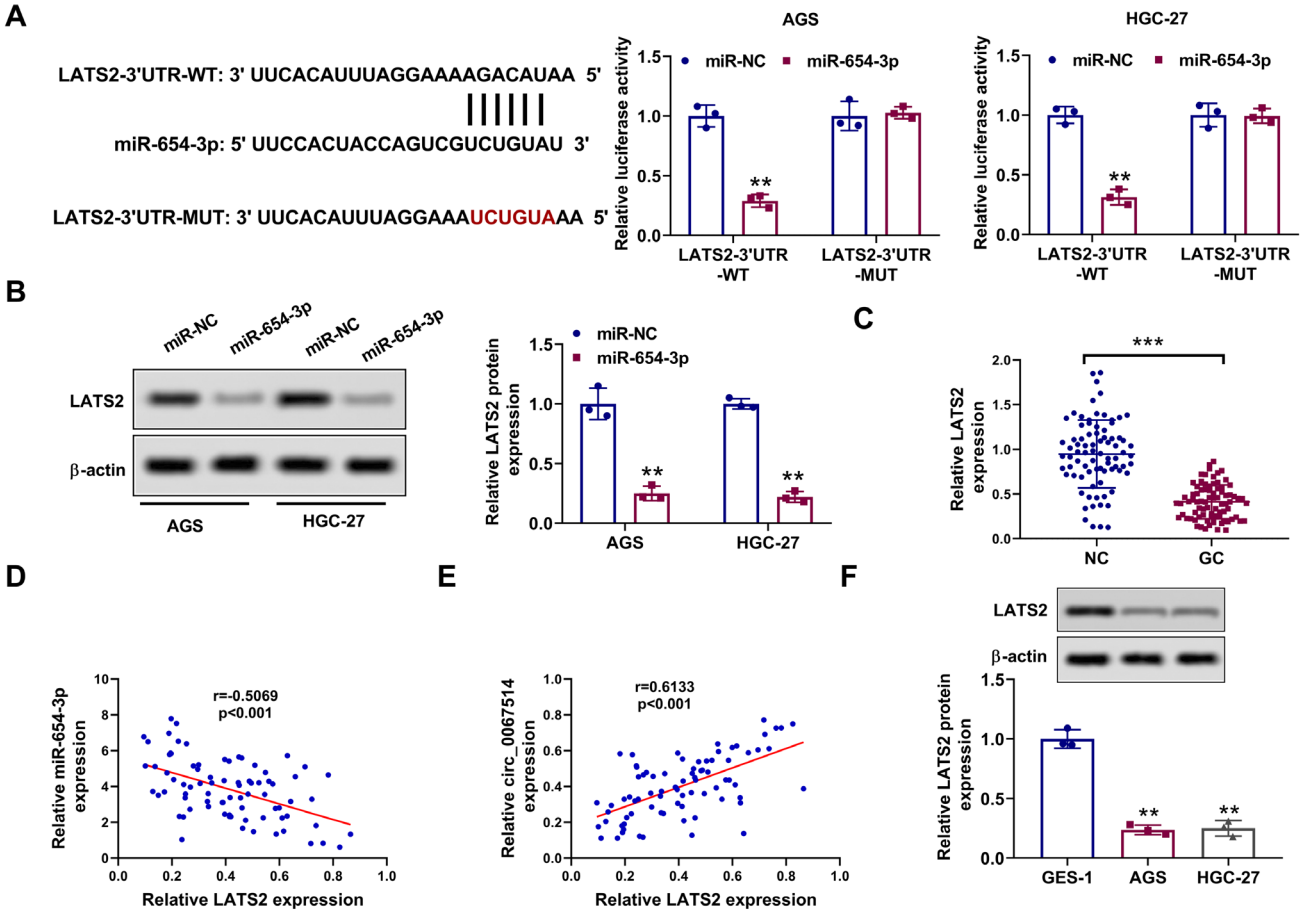

Figure 5. miR-654-3p targets LATS2. A) The putative targeting sites between miR-654-3p and LATS2 were presented, and the target relationship of miR-654-3p and LATS2 was verified by luciferase assay. **p<0.01 versus miR-NC group. B) The protein level of LATS2 in AGS and HGC-27 cells after transfection with miR-654-3p mimic was measured by western blot. **p<0.01 versus the miR-NC group. C) The expression of LATS2 mRNA in 80 gastric cancer patients was determined by qRT-PCR. ***p<0.001 versus the NC group. D) The association between miR-654-3p and LATS2 was analyzed by Pearson's correlation coefficient. E) Pearson's correlation coefficient analyzed the association between the expression of circ_0067514 and LATS2 in gastric cancer patients. F) The protein level of LATS2 in AGS and HGC-27 cells was measured by western blot. **p<0.01 versus GES-1.

→ Figure 6. circ_0067514 regulates gastric cancer progression via the miR-654-3p/LATS2 axis. A) The protein level of LATS2 in AGS and HGC-27 cells after transfection with si-LATS2 was assessed using a western blot. *p<0.05; **p<0.01 versus the si-NC group. B, C) The protein level of LATS2 in AGS and HGC-27 cells after co-transfection with pLCDH-circ_0067514 and miR-654-3p mimic or si-LATS2 was assessed using western blot. **p<0.01 versus the pLCDH-cir group. #p<0.05 versus the pLCDH-circ_0067514 group. D) Cell viability of AGS and HGC-27 after co-transfection with pLCDH-circ_0067514 and miR-654-3p mimic or si-LATS2 was evaluated using the CCK-8 assay. *p<0.05; **p<0.01. E, F) The proliferation ability of AGS and HGC-27 cells after co-transfection with pLCDH-circ_0067514 and miR-654-3p mimic or si-LATS2 was assessed by EdU staining. **p<0.01 versus the pLCDH-cir group. #p<0.05 versus the pLCDH-circ_0067514 group. G) Cell invasion of AGS and HGC-27 after co-transfection with pLCDH-circ_0067514 and miR-654-3p mimic or si-LATS2 was measured by Transwell invasion assay. **p<0.01 versus the pLCDH-cir group. #p<0.05 versus the pLCDH-circ_0067514 group. H) The protein levels of HK2 and LDHA in AGS and HGC-27 cells after co-transfection with pLCDH-circ_0067514 and miR-654-3p mimic or si-LATS2 were detected by western blot. **p<0.01 versus the pLCDH-cir group. #p<0.05 versus the pLCDH-circ_0067514 group.

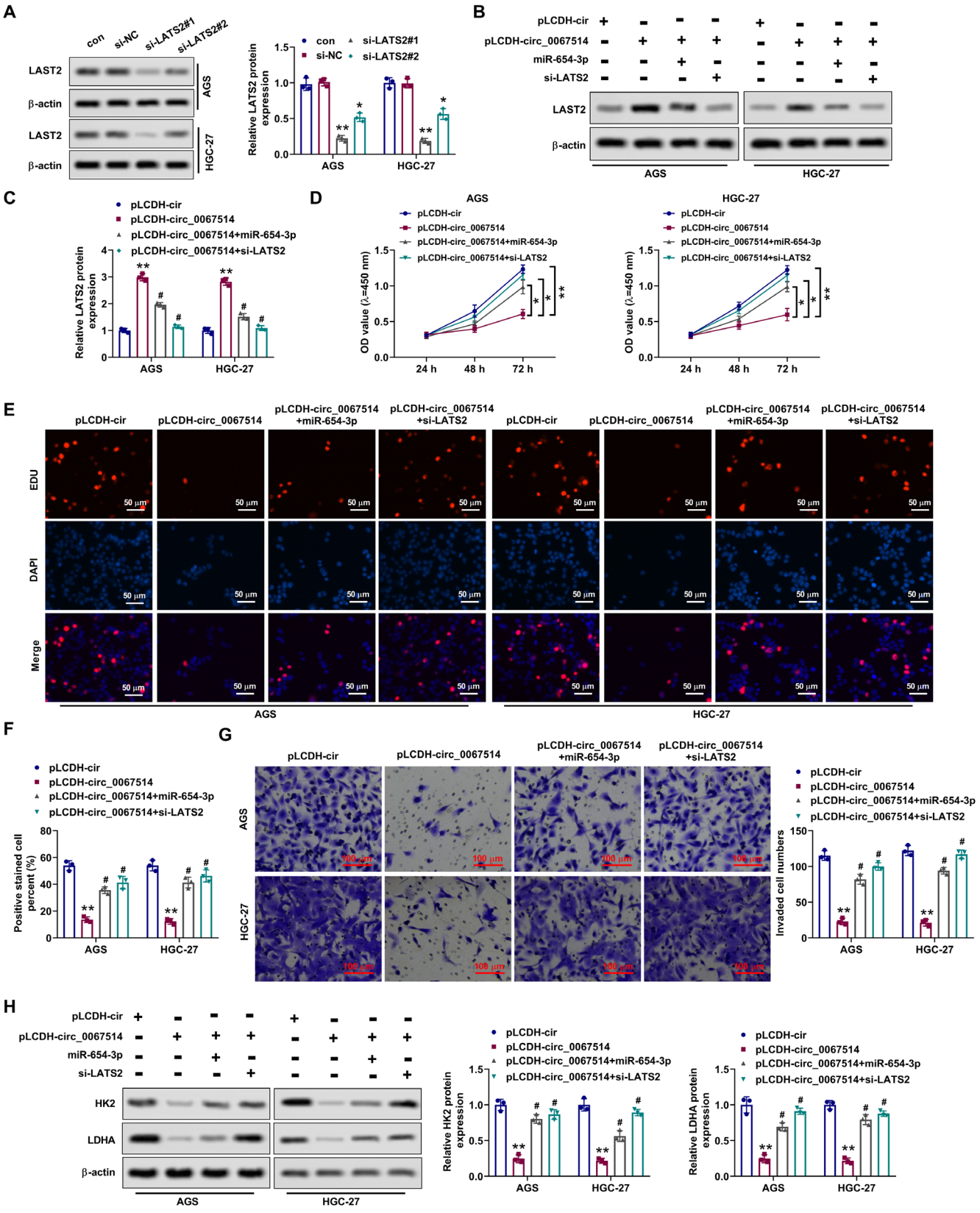
A
con
si-NC
si-LATS2#1
si-LATS2#2
LAST2
β-actin
AGS
HGC-27
Relative LATS2 protein expression
B
pLCDH-cir
pLCDH-circ_0067514
miR-654-3p
si-LATS2
C
pLCDH-cir
pLCDH-circ_0067514
pLCDH-circ_0067514+miR-654-3p
pLCDH-circ_0067514+si-LATS2
Relative LATS2 protein expression
D
OD value (λ=450 nm)
24 h
48 h
72 h
E
EDU
DAPI
Merge
50 μm
F
Positive stained cell percent (%)
G
100 μm
Invaded cell numbers
H
HK2
LDHA
Relative HK2 protein expression
Relative LDHA protein expression

Similar to the conclusion of *in vitro* studies, overexpression of circ_0067514 significantly suppressed tumor growth and tumor weight ($p<0.01$, Figures 7A and 7C), while did not interfere with the body weight ($p<0.01$, Figure 7B). Furthermore, the expression of circ_0067514 and LATS2 were elevated, and miR-654-3p was decreased in tumor tissues of mice with overexpression of circ_0067514 ($p<0.01$, Figure 7D). Immunohistochemistry revealed that Ki-67, N-cadherin, HK2, LDHA were decreased, and LATS2 and E-cadherin were increased in tumor tissues of mice with overexpression of circ_0067514 ($p<0.01$, Figure 7E). Taken together, circ_0067514 suppressed tumor growth of gastric cancer.

Discussion

Gastric cancer is the most common malignance with high prevalence and poor prognosis worldwide [1, 2, 8, 9]. Thus, it is imperative to fully clarify the mechanism of gastric cancer malignant development. Recently, accumulating evidence reveals the cancer modulation function of circRNAs [23]. However, only a few circRNAs have been well identified in gastric cancer so far. Hence, we studied the role of hsa_circ_0067514 in gastric cancer and found that hsa_circ_0067514 suppressed gastric cancer development and glycolysis through the miR-654-3p/LATS2 axis.

To investigate the action of hsa_circ_0067514 on gastric cancer, its expression was first verified. According to the bioinformatics analysis results based on GSE184882 and qRT-PCR results of gastric cancer patients and cells, we observed that circ_0067514 was lowly expressed in gastric cancer. So far, this study has firstly reported the abnormal expression of circ_0067514 in gastric cancer. Notably, the circ_0067514 expression was correlated with the overall survival, lymph node metastasis, TNM stage, and histological differentiation of gastric cancer. Similarly, CEP70, the host gene of circ_0067514, was associated with histological grade, TNM stage, and lymph node metastasis of pancreatic cancer [24]. These findings indicated the possibility that circ_0067514 is involved in regulating gastric cancer malignant development.

The expression of circ_0067514 was enforced in gastric cancer cells to clarify the role of circ_0067514 in gastric cancer. It was shown that overexpression of circ_0067514 blocked the proliferation and invasion of gastric cancer cells. Due to the EMT process playing crucial roles in tumor aggressive behavior [25], the action of circ_0067514 on EMT was studied by detecting the expression of E-cadherin and N-cadherin. Ki-67 expression was related to the EMT process, and Ki-67 might induce EMT by increasing vimentin expression [26–28]. Therefore, the expression of Ki-67 also was detected. We found that overexpression of circ_0067514 suppressed the EMT process of gastric cancer cells. Up to now, this study has first discovered the role of circ_0067514 in suppressing gastric cancer proliferation, invasion, and EMT.

It is generally accepted that metabolic reprogramming exists in cancer cells to provide sufficient energy for rapid biosynthesis [29]. The metabolic reprogramming phenomenon is aerobic glycolysis or the "Warburg effect" [30], featuring reinforced glycolysis under normoxia [31]. The "Warburg effect" of cancer cells exhibits enhanced glucose consumption, glycolytic activity, and accumulation of lactic acid [32]. Hence, inhibition of glycolysis was considered a potential therapeutic strategy for cancer. Accumulating evidence reveals that glycolysis also plays a critical role in gastric cancer [31, 32]. Shao et al. proved that spalt like transcription factor 4 (SALL4) promoted gastric cancer development via modulating glycolysis [33]. We, therefore, investigated whether circ_0067514 regulated glycolysis in gastric cancer and found that overexpression of circ_0067514 suppressed glucose absorption, lactate formation, and ATP level. Thus, overexpression of circ_0067514 restricted glycolysis in gastric cancer.

CircRNAs regulate the progression of diseases through functioning as RBP sponges, gene transcription modulators, RNA splicing regulators, and miRNA sponges [10]. For miRNA sponges, circRNAs contain multiple MERs, making circRNAs serve as the ceRNAs to target miRNAs and control downstream gene expression [11]. To study the precise molecular mechanism of circ_0067514 on gastric cancer proliferation, invasion, EMT, and glycolysis, the miRNA targeted by circ_0067514 was screened. According to the bioinformatics analysis results and experimental verification results, we found that circ_0067514 targeted miR-654-3p and circ_0067514 negatively regulated the miR-654-3p expression. Given that it was involved in regulating multiple cancer progression processes [34, 35], miR-654-3p was considered a momentous miRNA. In non-small cell lung cancer (NSCLC), miR-654-3p inhibits tumor growth [34]. In hepatocellular carcinoma, miR-654-3p suppresses cell aggressive behaviors [35]. Significantly, miR-654-3p is upregulated in gastric cancer and participates in gastric cancer tumorigenesis [20, 36]. In this research, miR-654-3p presented high expression in gastric cancer, which was in compliance with the previous study [20]. Furthermore, Hu et al. found that miR-654-3p was regulated by hsa_circ_0079480 and modulated tumor growth and cell apoptosis of acute myeloid leukemia [37]. Deng et al. revealed that miR-654-3p was absorbed by circRHOBTB3 to modulate gastric cancer growth [20]. In this study, circ_0067514 functioned as a miR-654-3p sponge to regulate gastric cancer development.

miRNAs function as negative gene modulators to suppress the target gene expression [38]. For example, overexpression of miR-129-5p contributes to etoposide-induced lung cancer apoptosis by suppressing the YWHAB expression [39]. Therefore, the target gene of miR-654-3p was searched. Results discovered that miR-654-3p targeted LATS2 and negatively regulated the LATS2 expression. LATS2 is proven to exert tumor suppressor function in cancers [40, 41]. For example, overexpression of LATS2 induces cell apoptosis

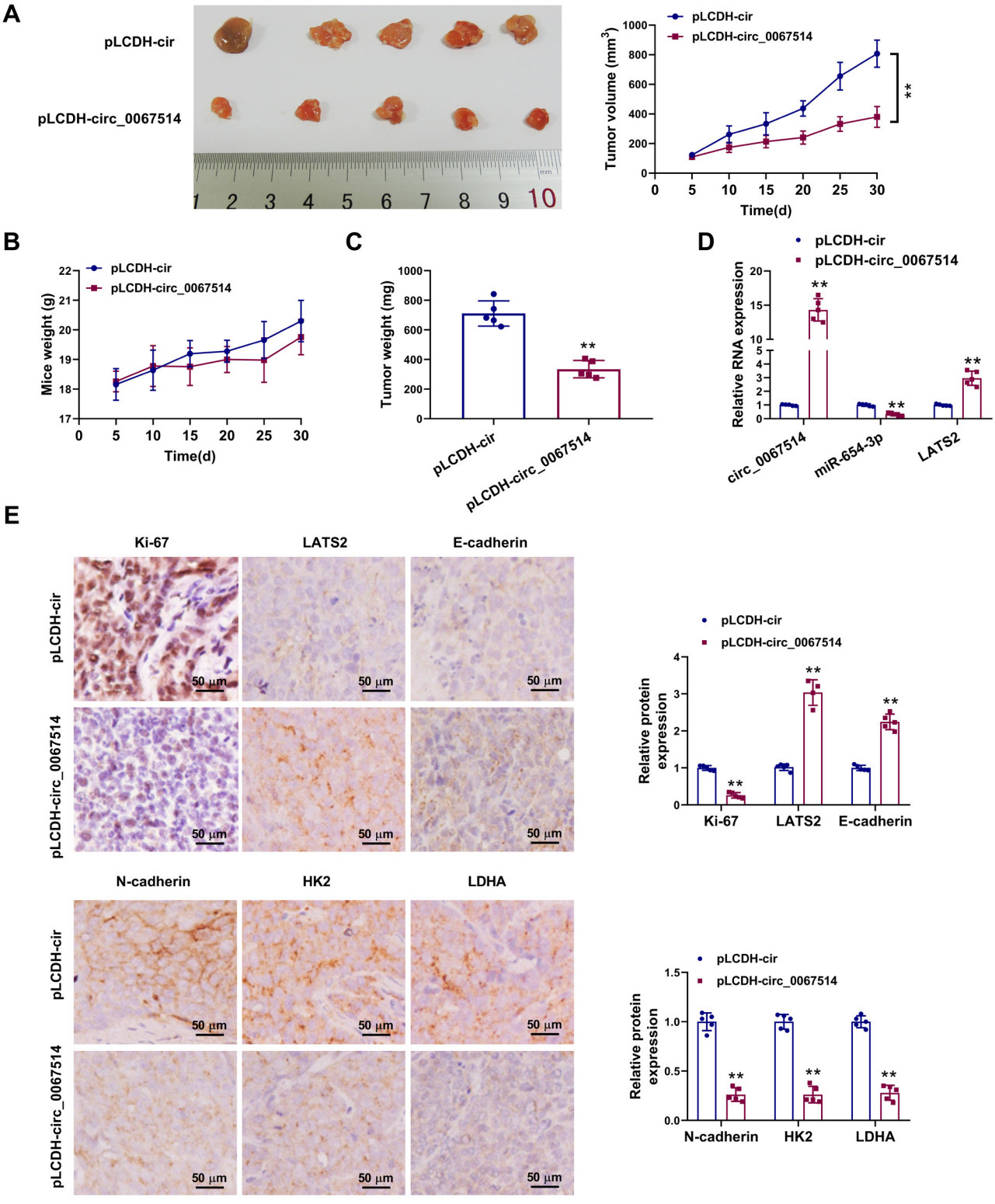

Figure 7. circ_0067514 blocks tumor growth of gastric cancer *in vivo*. A) The images of xenografts from mice injected with pLCDH-cir/AGS and pLCDH-circ_0067514/AGS, and the tumor volume was recorded. B) The body weight of mice injected with pLCDH-cir/AGS and pLCDH-circ_0067514/AGS was measured. C) The tumor weight of mice injected with pLCDH-cir/AGS and pLCDH-circ_0067514/AGS was measured. D) The expression levels of circ_0067514, miR-654-3p, and LATS2 in tumor tissues were detected by qRT-PCR. E) The levels of Ki-67, LATS2, E-cadherin, N-cadherin, HK2, and LDHA in tumor tissues were determined by immunohistochemistry. **p<0.01 versus the pLCDH-cir group.

in NSCLC [40]. In breast cancer, LATS2 suppresses cancer progression by maintaining cell identity and metabolic state [41]. LATS2 also participates in gastric cancer proliferation and invasion [42, 43]. This study found that LATS2 was downregulated in gastric cancer. The finding was consistent with the previous study [44]. Furthermore, Cho et al. found that LATS2 was targeted by miR-372 and regulated gastric cancer cell cycle and apoptosis [45]. Li et al. found that miR-93-5p promoted gastric cancer development via targeting LATS2 [46]. Moreover, LATS2 participated in the regulation of gastric cancer aggressive development in this study. Collectively, miR-654-3p targeted LATS2 to regulate gastric cancer development.

Together, circ_0067514 is downregulated in gastric cancer and blocks gastric cancer progression and glycolysis via the miR-654-3p/LATS2 axis. This paper reports the action of circ_0067514 on gastric cancer and the detailed mechanism for the first time. These findings make circ_0067514 a valuable therapeutic target against gastric cancer. Unfortunately, the small sample size was a limitation of the research. The study on large sample sizes of gastric cancer patients will be conducted in the future to clarify the significance of circ_0067514.

Acknowledgments: This study was supported by the grant: Scientific Research Project of Hunan Provincial Health Commission (C2019068).

References

[1] TSENG HH, CHEN YZ, CHOU NH, CHEN YC, WU CC et al. Metformin inhibits gastric cancer cell proliferation by regulation of a novel Loc100506691-CHAC1 axis. Mol Ther Oncolytics 2021; 22: 180–194. https://doi.org/10.1016/j.omto.2021.08.006

[2] SIEGEL RL, MILLER KD, JEMAL A. Cancer statistics, 2015. CA Cancer J Clin 2015; 65: 5–29. https://doi.org/10.3322/caac.21254

[3] DAI XM, ZHANG YH, LIN XH, HUANG XX, ZHANG Y et al. SIK2 represses AKT/GSK3β/β-catenin signaling and suppresses gastric cancer by inhibiting autophagic degradation of protein phosphatases. Mol Oncol 2021; 15: 228–245. https://doi.org/10.1002/1878-0261.12838

[4] BRAY F, FERLAY J, SOERJOMATARAM I, SIEGEL RL, TORRE LA et al. Global cancer statistics 2018: GLOBOCAN estimates of incidence and mortality worldwide for 36 cancers in 185 countries. CA Cancer J Clin 2018; 68: 394–424. https://doi.org/10.3322/caac.21492

[5] LUO Z, RONG Z, ZHANG J, ZHU Z, YU Z et al. Circular RNA circCCDC9 acts as a miR-6792-3p sponge to suppress the progression of gastric cancer through regulating CAV1 expression. Mol Cancer 2020; 19: 86. https://doi.org/10.1186/s12943-020-01203-8

[6] MACONI G, MANES G, PORRO GB. Role of symptoms in diagnosis and outcome of gastric cancer. World J Gastroenterol 2008; 14: 1149–1155. https://doi.org/10.3748/wjg.14.1149

[7] POWER DG, KELSEN DP, SHAH MA. Advanced gastric cancer--slow but steady progress. Cancer Treat Rev 2010; 36: 384–392. https://doi.org/10.1016/j.ctrv.2010.01.005

[8] ZHAO TT, XU H, XU HM, WANG ZN, XU YY et al. The efficacy and safety of targeted therapy with or without chemotherapy in advanced gastric cancer treatment: a network meta-analysis of well-designed randomized controlled trials. Gastric Cancer 2018; 21: 361–371. https://doi.org/10.1007/s10120-018-0813-2

[9] MA Y, REN Y, WEN H, CUI C. circCOL1A1 Promotes the Progression of Gastric Cancer Cells through Sponging miR-145 to Enhance RABL3 Expression. J Immunol Res 2021; 2021: 6724854. https://doi.org/10.1155/2021/6724854

[10] ZHENG X, HUANG M, XING L, YANG R, WANG X et al. The circRNA circSEPT9 mediated by E2F1 and EIF4A3 facilitates the carcinogenesis and development of triple-negative breast cancer. Mol Cancer 2020; 19: 73. https://doi.org/10.1186/s12943-020-01183-9

[11] YAN M, NIU L, LIU J, YAO Y, LI H. circEVI5 acts as a miR-4793-3p sponge to suppress the proliferation of gastric cancer. Cell Death Dis 2021; 12: 774. https://doi.org/10.1038/s41419-021-04061-4

[12] HAN B, CHAO J, YAO H. Circular RNA and its mechanisms in disease: From the bench to the clinic. Pharmacol Ther 2018; 187: 31–44. https://doi.org/10.1016/j.pharmthera.2018.01.010

[13] HUANG XY, ZHANG PF, WEI CY, PENG R, LU JC et al. Circular RNA circMET drives immunosuppression and anti-PD1 therapy resistance in hepatocellular carcinoma via the miR-30-5p/snail/DPP4 axis. Mol Cancer 2020; 19: 92. https://doi.org/10.1186/s12943-020-01213-6

[14] ZENG L, LIU YM, YANG N, ZHANG T, XIE H. Hsa_circRNA_100146 Promotes Prostate Cancer Progression by Upregulating TRIP13 via Sponging miR-615-5p. Front Mol Biosci 2021; 8: 693477. https://doi.org/10.3389/fmolb.2021.693477

[15] ZHANG X, WANG S, WANG H, CAO J, HUANG X et al. Circular RNA circNRIP1 acts as a microRNA-149-5p sponge to promote gastric cancer progression via the AKT1/mTOR pathway. Mol Cancer 2019; 18: 20. https://doi.org/10.1186/s12943-018-0935-5

[16] PENG L, SANG H, WEI S, LI Y, JIN D et al. circCUL2 regulates gastric cancer malignant transformation and cisplatin resistance by modulating autophagy activation via miR-142-3p/ROCK2. Mol Cancer 2020; 19: 156. https://doi.org/10.1186/s12943-020-01270-x

[17] WU K, YU Z. miR-877-5p Suppresses Gastric Cancer Cell Proliferation Through Targeting FOXM1. Onco Targets Ther 2020; 13: 4731–4742. https://doi.org/10.2147/OTT.S251916

[18] HE X, SHU Y. miR-452 promotes the development of gastric cancer via targeting EPB41L3. Pathol Res Pract 2020; 216: 152725. https://doi.org/10.1016/j.prp.2019.152725

[19] SALMENA L, POLISENO L, TAY Y, KATS L, PANDOLFI PP. A ceRNA hypothesis: the Rosetta Stone of a hidden RNA language? Cell 2011; 146: 353–358. https://doi.org/10.1016/j.cell.2011.07.014

[20] DENG G, MOU T, HE J, CHEN D, LV D et al. Circular RNA circRHOBTB3 acts as a sponge for miR-654-3p inhibiting gastric cancer growth. J Exp Clin Cancer Res 2020; 39: 1. https://doi.org/10.1186/s13046-019-1487-2

[21] GAO W, CHEN X, CHI W, XUE M. Long non-coding RNA MKLN1-AS aggravates hepatocellular carcinoma progression by functioning as a molecular sponge for miR-654-3p, thereby promoting hepatoma-derived growth factor expression. Int J Mol Med 2020; 46: 1743–1754. https://doi.org/10.3892/ijmm.2020.4722

[22] YAO F, LIU H, LI Z, ZHONG C, FANG W. Down-regulation of LATS2 in non-small cell lung cancer promoted the growth and motility of cancer cells. Tumor Biology 2015; 36: 2049–2057. https://doi.org/10.1007/s13277-014-2812-1

[23] MENG S, ZHOU H, FENG Z, XU Z, TANG Y et al. CircRNA: functions and properties of a novel potential biomarker for cancer. Mol Cancer 2017; 16: 94. https://doi.org/10.1186/s12943-017-0663-2

[24] XIE S, QIN J, LIU S, ZHANG Y, WANG J et al. Cep70 overexpression stimulates pancreatic cancer by inducing centrosome abnormality and microtubule disorganization. Sci Rep 2016; 6: 21263. https://doi.org/10.1038/srep21263

[25] RIBATTI D, TAMMA R, ANNESE T. Epithelial-Mesenchymal Transition in Cancer: A Historical Overview. Transl Oncol 2020; 13: 100773. https://doi.org/10.1016/j.tranon.2020.100773

[26] TIAN Y, MA Z, CHEN Z, LI M, WU Z et al. Clinicopathological and Prognostic Value of Ki-67 Expression in Bladder Cancer: A Systematic Review and Meta-Analysis. PLoS One 2016; 11: e0158891. https://doi.org/10.1371/journal.pone.0158891

[27] YU JQ, ZHOU Q, ZHENG YF, BAO Y. Expression of Vimentin and Ki-67 Proteins in Cervical Squamous Cell Carcinoma and their Relationships with Clinicopathological Features. Asian Pac J Cancer Prev 2015; 16: 4271–4275. https://doi.org/10.7314/apjcp.2015.16.10.4271

[28] PENG H, TAN X, WANG Y, DAI L, LIANG G et al. Clinical significance of Ki67 and circulating tumor cells with an epithelial-mesenchymal transition phenotype in non-small cell lung cancer. Am J Transl Res 2020; 12: 2916–2928.

[29] VANDER HEIDEN MG, CANTLEY LC, THOMPSON CB. Understanding the Warburg effect: the metabolic requirements of cell proliferation. Science 2009; 324: 1029–1033. https://doi.org/10.1126/science.1160809

[30] WARBURG O. On the origin of cancer cells. Science 1956; 123: 309–314. https://doi.org/10.1126/science.123.3191.309

[31] YU S, HU C, CAI L, DU X, LIN F et al. Seven-Gene Signature Based on Glycolysis Is Closely Related to the Prognosis and Tumor Immune Infiltration of Patients With Gastric Cancer. Front Oncol 2020; 10: 1778. https://doi.org/10.3389/fonc.metabolism in gastric cancer: The cutting-edge. World J Gastroenterol 2016; 22: 2046–2059. https://doi.org/10.3748/wjg.v22.i6.2046

[33] SHAO M, ZHANG J, ZHANG J, SHI H, ZHANG Y et al. SALL4 promotes gastric cancer progression via hexokinase II mediated glycolysis. Cancer Cell Int 2020; 20: 188. https://doi.org/10.1186/s12935-020-01275-y

[32] YUAN LW, YAMASHITA H, SETO Y. Glucose metabolism in gastric cancer: The cutting-edge. World J Gastroenterol 2016; 22: 2046–2059. https://doi.org/10.3748/wjg.v22.i6.2046

[34] PU JT, HU Z, ZHANG DG, ZHANG T. MiR-654-3p Suppresses Non-Small Cell Lung Cancer Tumourigenesis by Inhibiting PLK4. Onco Targets Ther 2020; 13: 7997–8008. https://doi.org/10.2147/OTT.S258616

[35] YANG J, ZHANG Z, CHEN S, DOU W, XIE R et al. miR-654-3p predicts the prognosis of hepatocellular carcinoma and inhibits the proliferation, migration, and invasion of cancer cells. Cancer Biomark 2020; 28: 73–79. https://doi.org/10.3233/CBM-191084

[36] GAO W, CHEN X, CHI W, XUE M. Long non-coding RNA MKLN1-AS aggravates hepatocellular carcinoma progression by functioning as a molecular sponge for miR-654-3p, thereby promoting hepatoma-derived growth factor expression. Int J Mol Med 2020; 46: 1743–1754. https://doi.org/10.3892/ijmm.2020.4722

[37] HU Q, GU Y, CHEN S, TIAN Y, YANG S. Hsa_circ_0079480 promotes tumor progression in acute myeloid leukemia via miR-654-3p/HDGF axis. Aging (Albany NY) 2020; 13: 1120–1131. https://doi.org/10.18632/aging.202240

[38] ACHKAR NP, CAMBIAGNO DA, MANAVELLA PA. miRNA Biogenesis: A Dynamic Pathway. Trends Plant Sci 2016; 21: 1034–1044. https://doi.org/10.1016/j.tplants.2016.09.003

[39] XU C, DU Z, REN S, LIANG X, LI H. MiR-129-5p sensitization of lung cancer cells to etoposide-induced apoptosis by reducing YWHAB. J Cancer 2020; 11: 858–866. https://doi.org/10.7150/jca.35410

[40] XIE Y, LV Y, ZHANG Y, LIANG Z, HAN L et al. LATS2 promotes apoptosis in non-small cell lung cancer A549 cells via triggering Mff-dependent mitochondrial fission and activating the JNK signaling pathway. Biomed Pharmacother 2019; 109: 679–689. https://doi.org/10.1016/j.biopha.2018.10.097

[41] FURTH N, PATERAS IS, ROTKOPF R, VLACHOU V, RIVKIN I et al. LATS1 and LATS2 suppress breast cancer progression by maintaining cell identity and metabolic state. Life Sci Alliance 2018; 1: e201800171. https://doi.org/10.26508/lsa.201800171

[42] WANG YJ, LIU JZ, LV P, DANG Y, GAO JY et al. Long non-coding RNA CCAT2 promotes gastric cancer proliferation and invasion by regulating the E-cadherin and LATS2. Am J Cancer Res 2016; 6: 2651–2660.

[43] ZHANG Y, HE LJ, HUANG LL, YAO S, LIN N et al. Oncogenic PAX6 elicits CDK4/6 inhibitor resistance by epigenetically inactivating the LATS2-Hippo signaling pathway. Clin Transl Med 2021; 11: e503. https://doi.org/10.1002/ctm2.503

[44] MATSUI S, KAGARA N, MISHIMA C, NAOI Y, SHIMODA M et al. LATS2 promoter hypermethylation and its effect on gene expression in human breast cancer. Oncol Lett 2018; 15: 2595–2603. https://doi.org/10.3892/ol.2017.7535

[45] CHO WJ, SHIN JM, KIM JS, LEE MR, HONG KS et al. miR-372 regulates cell cycle and apoptosis of ags human gastric cancer cell line through direct regulation of LATS2. Mol Cells 2009; 28: 521–527. https://doi.org/10.1007/s10059-009-0158-0

[46] LI L, ZHAO J, HUANG S, WANG Y, ZHU L et al. MiR-93-5p promotes gastric cancer-cell progression via inactivation of the Hippo signaling pathway. Gene 2018; 641: 240–247. https://doi.org/10.1016/j.gene.2017.09.071